IMMUNOLOGY

Dimerization of the adaptor Gads facilitates antigen receptor signaling by promoting the cooperative binding of Gads to the adaptor LAT

Sigalit Sukenik,[1] Maria P. Frushicheva,[2] Cecilia Waknin-Lellouche,[1] Enas Hallumi,[1] Talia Ifrach,[1] Rose Shalah,[1] Dvora Beach,[1] Reuven Avidan,[1] Ilana Oz,[1] Evgeny Libman,[1]* Ami Aronheim,[3] Oded Lewinson,[4] Deborah Yablonski[1†]

The accurate assembly of signalosomes centered on the adaptor protein LAT (linker of activated T cells) is required for antigen receptor signaling in T cells and mast cells. During signalosome assembly, members of the growth factor receptor–bound protein 2 (Grb2) family of cytosolic adaptor proteins bind cooperatively to LAT through interactions with its phosphorylated tyrosine (pTyr) residues. We demonstrated the Src homology 2 (SH2) domain–mediated dimerization of the Grb2 family member, Grb2-related adaptor downstream of Shc (Gads). Gads dimerization was mediated by an SH2 domain interface, which is distinct from the pTyr binding pocket and which promoted cooperative, preferential binding of paired Gads to LAT. This SH2 domain–intrinsic mechanism of cooperativity, which we quantified by mathematical modeling, enabled Gads to discriminate between dually and singly phosphorylated LAT molecules. Mutational inactivation of the dimerization interface reduced cooperativity and abrogated Gads signaling in T cells and mast cells. The dimerization-dependent, cooperative binding of Gads to LAT may increase antigen receptor sensitivity by reducing signalosome formation at incompletely phosphorylated LAT molecules, thereby prioritizing the formation of complete signalosomes.

INTRODUCTION

Antigen recognition stimulates similar signaling pathways in T cells and mast cells. Upon antigen recognition, both the T cell receptor (TCR) and the mast cell high-affinity immunoglobulin E (IgE) receptor (FcεRI) stimulate ITAM (immunoreceptor tyrosine-based activation motif)–dependent signaling cascades (*1*), which are initiated by Src and Syk family tyrosine kinases (*2*, *3*). The Syk family kinase directly phosphorylates two key adaptor proteins: linker of activated T cells (LAT), a membrane-bound adaptor; and Src homology 2 (SH2) domain–containing leukocyte protein of 76 kDa (SLP-76), a cytoplasmic adaptor (*2*). LAT is phosphorylated at multiple tyrosine residues, which stimulates the SH2 domain–mediated assembly of large LAT-nucleated signaling complexes (*4*–*8*). Among the proteins recruited to LAT are the growth factor receptor–bound protein 2 (Grb2) family adaptor proteins Grb2, Grap (Grb2-related adapter protein), and Gads (Grb2-related adaptor downstream of Shc) (*9*, *10*). Grb2 proteins are composed of a central SH2 domain that is flanked by two SH3 domains as well as a unique proline-rich linker that is found only in Gads. Located in the cytoplasm, Grb2 proteins bind to key signaling proteins through their SH3 domains. Grb2 binds constitutively to Son of Sevenless (SOS), whereas the C-terminal SH3 domain of Gads binds with high affinity to an RAK motif in SLP-76 (*11*–*13*). The central SH2 domain of Grb2 family proteins is specific for phospho-YxN (pYxN) motifs, at least three of which are found in LAT. In this way, Grb2 recruits SOS to LAT, whereas Gads recruits SLP-76 to LAT. Phospholipase C–γ1 (PLC-γ1) binds directly to phosphorylated LAT (pLAT) and is phosphorylated and activated by the SLP-76–associated tyrosine kinase Itk (*14*, *15*) through a multistep mechanism that depends on the association of Itk with SLP-76 (*16*, *17*). Gads facilitates the phosphorylation of PLC-γ1 by bridging the binding of SLP-76 to LAT (*18*–*21*). Activated PLC-γ1 generates inositol 1,4,5-trisphosphate, which stimulates the increased intracellular calcium that is required for subsequent transcriptional changes. In murine bone marrow–derived mast cells (BMMCs), an increase in the concentration of intracellular calcium stimulates the rapid release of preformed allergic mediators through a process known as degranulation, which depends on LAT, Gads, and SLP-76 (*22*–*24*).

At least four tyrosine phosphorylation sites on LAT are required for the TCR-dependent activation of PLC-γ1: Tyr^{132}, Tyr^{171}, Tyr^{191}, and Tyr^{226} (*5*, *7*, *8*). PLC-γ1 binds selectively to ($pTyr^{132}$), whereas Gads and Grb2, by virtue of their similar SH2 domains, bind to pYxN motifs at Tyr^{171}, Tyr^{191}, and Tyr^{226} (*25*), suggesting that they may compete for binding sites on LAT. Both Tyr^{171} and Tyr^{191} are required for the stable binding of Gads to LAT and for downstream phosphorylation (and activation) of extracellular signal–regulated kinase and intracellular calcium mobilization (*5*, *8*). The requirement for dual binding sites is difficult to explain because Gads has only one SH2 domain, which has a single pTyr binding pocket. The binding of Gads to LAT is further increased when all three pYxN sites are present (*8*). These observations suggest the possibility of cooperative binding to LAT; however, the mechanism of cooperativity is unknown.

Gads-deficient mice exhibit a partial block in T cell development at the pre-TCR checkpoint as well as impairment of both positive and negative selection (*26*–*28*), whereas mice lacking LAT or SLP-76 exhibit a complete block in thymic development because of the abrogation of pre-TCR and TCR signaling (*29*–*31*). These differences are largely recapitulated in Jurkat-derived T cell lines that lack LAT (J.Cam2), SLP-76 (J14), or Gads (dG32). LAT- and SLP-76–deficient T cell lines exhibit profoundly impaired TCR-stimulated intracellular calcium mobilization and impaired TCR-induced transcriptional responses (*32*, *33*), whereas the Gads-deficient cells have a reduced amplitude of TCR

[1]Department of Immunology, Ruth and Bruce Rappaport Faculty of Medicine, Technion—Israel Institute of Technology, Haifa 3525433, Israel. [2]Department of Chemical Engineering, Massachusetts Institute of Technology, Cambridge, MA 02142, USA. [3]Department of Cell Biology and Cancer Science, Ruth and Bruce Rappaport Faculty of Medicine, Technion—Israel Institute of Technology, Haifa 3525433, Israel. [4]Department of Biochemistry, Ruth and Bruce Rappaport Faculty of Medicine, Technion—Israel Institute of Technology, Haifa 3525433, Israel.
*Present address: MediWound Ltd., Yavne, Israel.
†Corresponding author. Email: debya@tx.technion.ac.il

responses (*21*, *34*). We hypothesized that the requirement of Gads for dual-LAT binding sites might promote antigen receptor responsiveness by selectively directing complex formation to LAT molecules that have accumulated multiple phosphorylation events. To explore the mechanistic basis for this requirement, we devised biochemical assays and a mathematical model, which describes the preferentially paired, cooperative binding of Gads to LAT molecules that are phosphorylated at both Tyr^{171} and Tyr^{191} (dual-pLAT). The Gads SH2 domain dimerization interface, as defined in this study, facilitated discrimination between single- and dual-pLAT molecules and was required for Gads signaling functions in T cells and mast cells.

RESULTS

Spontaneous dimerization of Gads through its SH2 domain

Gads contains a single SH2 domain, yet it requires two LAT pTyr sites for efficient binding (*8*). To explore this discrepancy, we resolved a recombinant maltose-binding protein (MBP)–Gads fusion protein by size exclusion chromatography, which separates proteins on the basis of their globular radius. Full-length Gads resolved into two main peaks (Fig. 1A), with elution volumes corresponding to the predicted molecular weight of monomeric and dimeric MBP-Gads (fig. S1A). SDS–polyacrylamide gel electrophoresis (SDS-PAGE) confirmed that both peaks contained an identical protein species, at the expected molecular weight of MBP-Gads (fig. S1B, left). To rule out partial protein unfolding as the source of either peak, we measured the protein denaturation temperature (T_m) by nano–differential scanning fluorimetry (nanoDSF), a technique in which proteins are gradually heated while the shift in intrinsic tryptophan fluorescence that occurs upon their unfolding is measured (*35*). Both peaks exhibited T_m values in the range of 56.5° to 56.7°C (Fig. 1B), suggesting that they represent alternative, stably folded conformations of MBP-Gads protein. Size exclusion chromatography and multiangle light scattering (SEC-MALS) confirmed that the earlier-eluting peak had twice the molecular weight of the later peak (fig. S1C, left), suggesting that it represents a spontaneously dimerized form of Gads.

The N- and C-terminal SH3 domains and the linker region of Gads (Fig. 1C) were not required for its resolution into two peaks (fig. S1D); purified MBP-SH2 resolved to two peaks (fig. S1D) at the expected sizes of its monomeric and dimeric forms (fig. S1A), with the earlier peak exhibiting a SEC-MALS signal corresponding to the dimeric form (fig. S1C, right). The MBP tag facilitated the purification and storage of recombinant Gads proteins but was not required for dimerization because a His-tagged Gads SH2 domain was resolved by size exclusion chromatography into two peaks (Fig. 1D) that exhibited identical mobility by SDS-PAGE (fig. S1B, right). These results suggest that spontaneous dimerization is an intrinsic property of the Gads SH2 domain.

To assess the stability of spontaneous Gads dimers, MBP-Gads proteins from the dimeric fraction were stored on ice or incubated at 37°C, and the resulting oligomerization state was determined by size exclusion chromatography. Full-length Gads protein from the dimeric fraction reequilibrated on ice to a mixture of monomeric and dimeric forms; however, a substantial fraction remained dimeric even after 2.5 hours at 37°C (Fig. 1E, left), suggesting that spontaneously formed Gads dimers were relatively stable at a physiologic temperature. In contrast, the isolated Gads SH2 domain converted rapidly to the monomeric form at 37°C (Fig. 1E, right), suggesting that additional Gads domains were required to stabilize the dimeric conformation at a physiologic temperature.

Nano-DSF analysis, which detects the increased solvent exposure of tryptophan residues as proteins unfold (*35*), may also be affected by the shielding of tryptophan residues upon domain dimerization. Consistent with this idea, nano-DSF analysis of the dimeric, His-tagged Gads SH2 domain revealed two temperature-dependent transitions (Fig. 1F). The first occurred at 32.5°C and was not associated with protein aggregation, suggesting that it represents the temperature of monomerization. A second transition, in the range of 54° to 57°C, was observed for both monomeric and dimeric Gads SH2 domains and was accompanied by protein aggregation, suggesting that it represents the T_m (Fig. 1F). A similar low-temperature transition was observed in the nano-DSF profile of the dimeric MBP-Gads SH2 domain (fig. S2); this transition was subtle, likely because of the presence of eight additional tryptophan residues in the MBP tag that are not affected by SH2 dimerization. Together, these data demonstrate that the earlier-eluting Gads SH2 domain peak represents a well-folded, spontaneously dimerized form, which dissociates to a well-folded monomeric form at about 32°C.

To confirm the self-association of full-length Gads at a physiologic temperature, we turned to the Ras recruitment system (RRS), a type of yeast two-hybrid system, in which the interaction of bait and prey proteins is required for yeast growth at the restrictive temperature (*36*). Growth was observed when full-length Gads was used both as bait and prey (Fig. 1G, row 2), but no growth occurred when either the bait or prey was eliminated (Fig. 1G, rows 1 and 3). Because this assay is performed at 36°C, it suggests that the self-association of full-length Gads occurs at a physiologic temperature and therefore may regulate its signaling function within cells.

Identification of the dimerization interface of the Gads SH2 domain

While examining a previously determined structure of the murine Gads SH2 domain cocrystallized with a short pLAT peptide [Protein Data Bank (PDB): 1R1P)] (*37*), we noted that the minimal asymmetric unit included two pairs of closely associated Gads SH2 domains, each bound to a pLAT peptide (Fig. 2A, left). A space-filling model demonstrates a tight association at the putative SH2 dimerization interface (fig. S3, top), which features an area of about 850 $Å^2$ (fig. S3, bottom), which is within the range of known dimerization interfaces (*38*). Within each pair, the two SH2 domains appear to be held together by hydrophobic interactions between F92 on adjacent domains as well as by hydrogen bonds between R109 on one partner and D91 on the other (Fig. 2A, right). Computational alanine scanning analysis of a dimeric model, based on a reconstituted Gads SH2 domain structure bound to short $pTyr^{171}$ and $pTyr^{191}$ peptides, predicted that mutation of Trp^{58}, Phe^{59}, Asp^{91}, Phe^{92}, Arg^{109}, or Tyr^{115} to alanine would destabilize the Gads SH2 domain dimer interface (Fig. 2B). Of these, the largest predicted destabilizing effect was for mutation of Phe^{92}. We attempted to disrupt the dimerization interface by mutating Phe^{92} and Arg^{109} in the context of MBP-Gads SH2. Single substitution of either residue with alanine was insufficient to disrupt dimerization (fig. S4), but the F92A,R109A double mutation completely disrupted spontaneous Gads SH2 domain dimerization (Fig. 2C). We reasoned that a more substantial disruptive effect might be obtained by the incorporation of a negative charge. Mutation of Arg^{109} to Asp was insufficient (fig. S4), but the F92D mutation completely abolished spontaneous Gads SH2 domain dimerization (Fig. 2C). In the context of full-length Gads, the F92D and F92A,R109A mutations abolished Gads dimerization (Fig. 2D) without adversely affecting the stability of protein folding (fig. S5).

Despite their marked effects on Gads dimerization, the F92D and F92A,R109A mutations only moderately reduced the affinity of Gads SH2 binding to a monophosphorylated LAT $pTyr^{171}$ peptide (Fig. 2E).

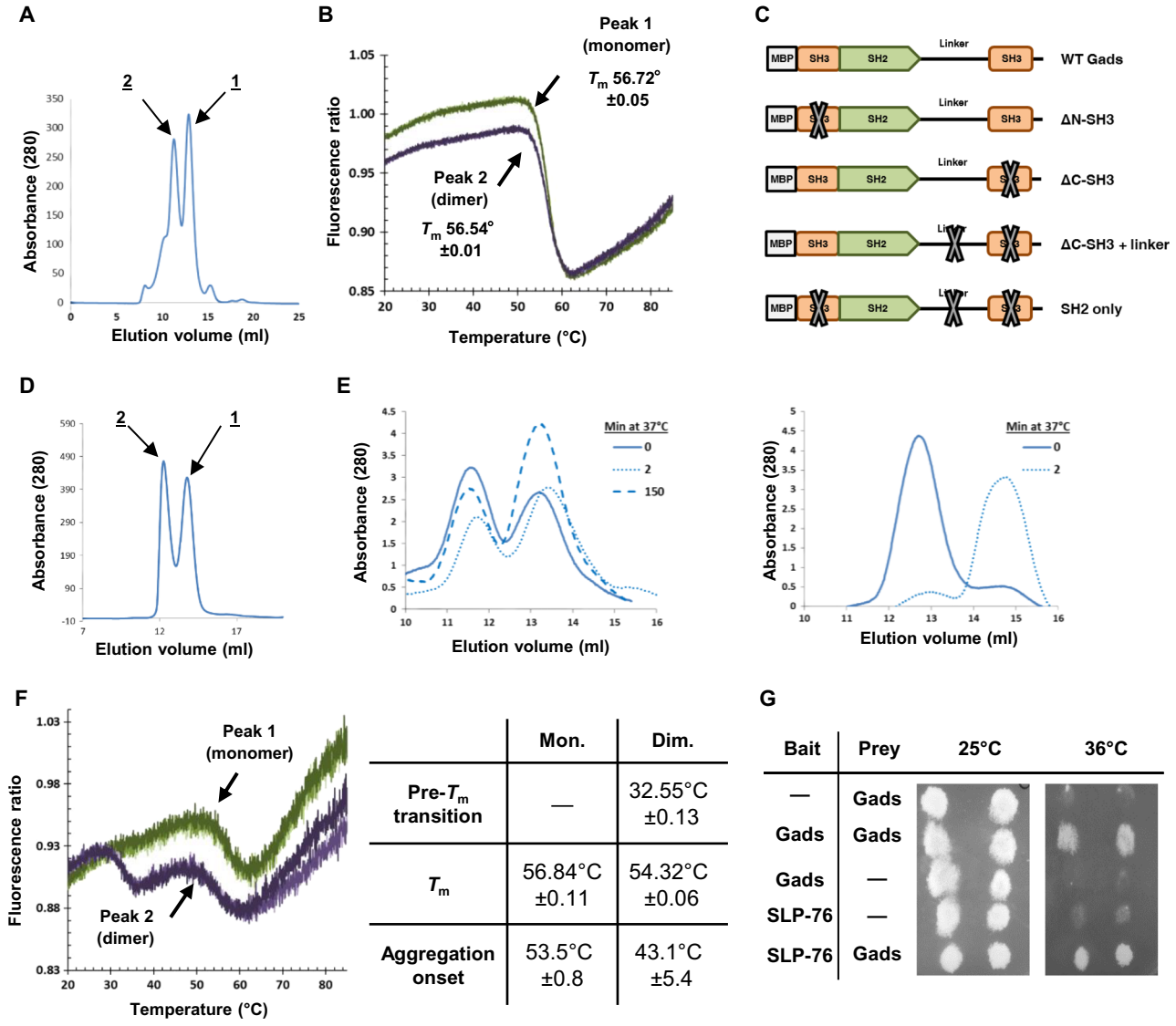

	Mon.	Dim.
Pre-T_m transition	—	32.55°C ±0.13
T_m	56.84°C ±0.11	54.32°C ±0.06
Aggregation onset	53.5°C ±0.8	43.1°C ±5.4

Fig. 1. Spontaneous Gads dimerization occurs through its SH2 domain. (**A**) Full-length MBP-Gads protein was resolved by size exclusion chromatography on a Superdex 200 10/300 GL column. The labeled peaks correspond to the monomer (1) and dimer (2). Data are representative of at least five independent experiments. (**B**) The thermal stability of purified MBP-Gads protein was determined by nano-DSF. Triplicate samples of MBP-Gads from peak 1 (monomer, green) and peak 2 (dimer, purple) were heated at a rate of 1°C/min while intrinsic tryptophan fluorescence was measured. The calculated T_m values are indicated. (**C**) Domain organization of wild-type (WT) and the indicated mutant MBP-Gads proteins. All constructs consistently resolved into two peaks (fig. S1D). (**D**) The His-tagged Gads SH2 domain was resolved by size exclusion chromatography on a Superdex 75 10/300 GL column. Peaks correspond to monomer (1) and dimer (2). Data are representative of at least three independent experiments. (**E**) Full-length MBP-Gads protein (left) or MBP-Gads SH2 domain protein (right) from the dimeric fraction shown in (D) was incubated at 37°C for the indicated times before undergoing size exclusion chromatography. Data are representative of three independent experiments. (**F**) Left: Triplicate samples of monomeric (peak 1, green) or dimeric (peak 2, purple) His-SH2 domain were analyzed by nano-DSF. Right: The resulting parameters of the monomer (Mon.) and dimer (Dim.). (**G**) Self-association of full-length Gads in yeast cells was demonstrated with the RRS, in which interaction of bait and prey proteins rescues yeast growth at the restrictive temperature of 36°C. The well-characterized interaction of Gads and SLP-76 served as a positive control. Data are representative of three independent experiments.

The WT Gads SH2 domain bound to pY171-LAT with a K_d (equilibrium dissociation constant) [$1/K_a$ (equilibrium association constant)] of 177 nM, which is within the range of previously reported values (*25*, *37*). Mutational inactivation of the dimerization interface moderately increased the K_d to 470 nM for the F92D mutant SH2 domain and 335 nM for the F92A, R109A SH2 domain mutant. These results are consistent with the proper folding of the SH2 domain and suggest that the Gads SH2 domain dimerization interface is largely distinct from the pTyr binding pocket. Together, our data identify an SH2 domain interface that is required for dimerization of the full-length Gads protein.

Preferentially paired binding of the Gads SH2 domain to its dual sites on LAT

We wondered whether transient Gads dimerization facilitated its cooperative binding to $pTyr^{171}$ and $pTyr^{191}$ on LAT (*8*). These sites are found at an evolutionarily conserved distance from each other and are connected by a highly conserved linker sequence (fig. S6, left boxed region), suggesting that they may function as a unit. To test this idea, we incubated the monomeric Gads SH2 domain with a molar excess of synthetic LAT peptide, encompassing both Gads binding sites, and phosphorylated at both (2pY-LAT) or one (pY171-LAT) of the sites

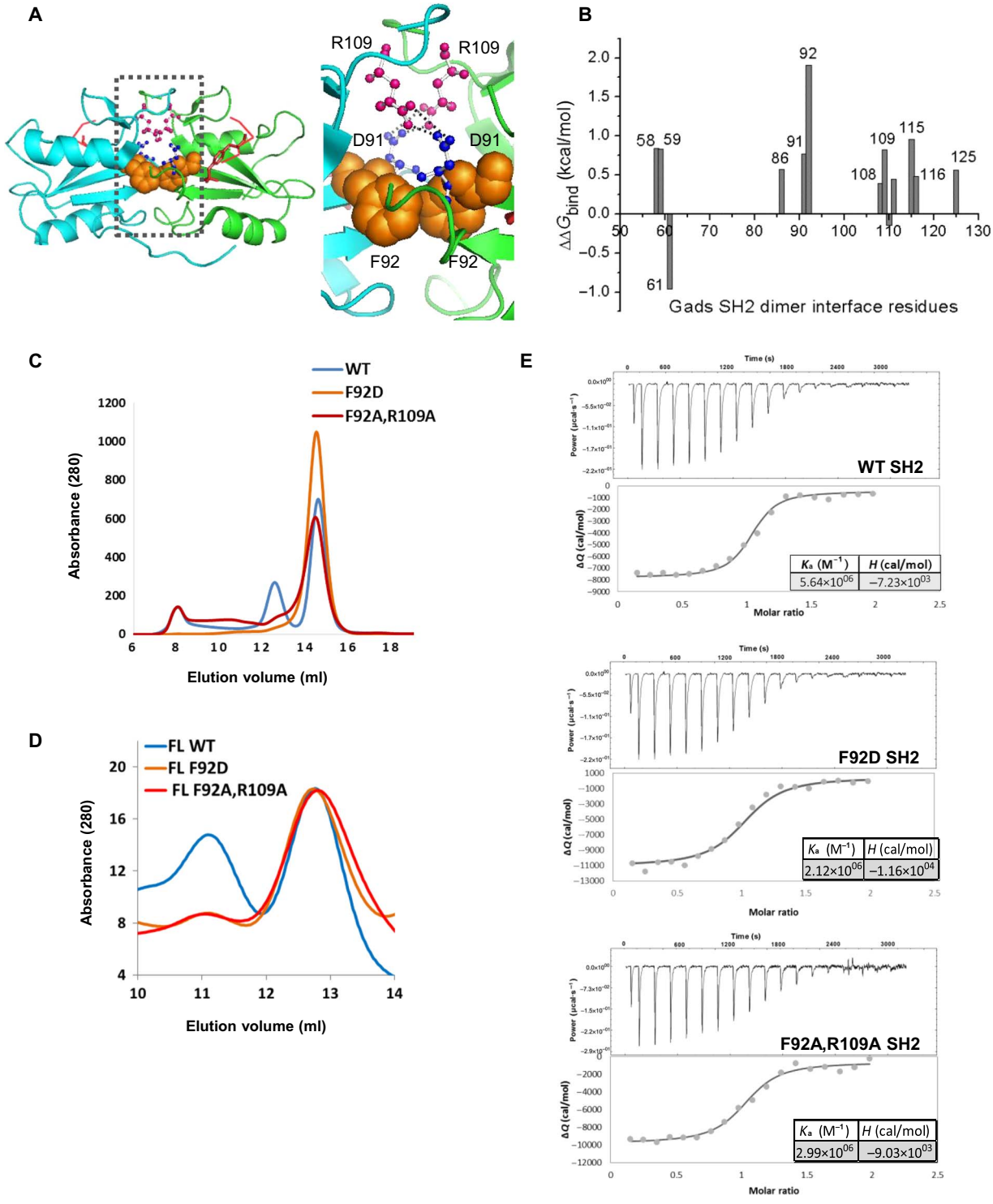

Fig. 2. Identification of the Gads SH2 domain dimerization interface. (**A**) Left: Structure of the murine Gads SH2 domain cocrystallized with a short peptide encompassing LAT-pY171 [PDB: 1R1P, (*37*)]. The adjacent SH2 units (cyan and green) are each bound to a pLAT peptide (red). The dotted box indicates the putative dimerization interface. Right: Enlarged view of part of the dimerization interface, highlighting the position of F92 (shown in space-filling form), D91, and R109. (**B**) The calculated binding free energy ($\Delta\Delta G_{bind}$) of amino acid residues that were predicted to destabilize ($\Delta\Delta G_{bind} > 0$) or stabilize ($\Delta\Delta G_{bind} < 0$) the Gads SH2 domain dimer interface when mutated to alanine, as determined by computational alanine scanning. (**C** and **D**) Purified MBP-Gads proteins bearing the indicated point mutations in either the SH2 domain alone (C) or the full-length (FL) Gads protein (D) were resolved by size exclusion chromatography. Data are representative of three independent experiments. (**E**) Representative isotherms for the interaction of the indicated monomeric MBP-Gads SH2 domains with the pY171-LAT peptide. Data analysis was performed with AFFINImeter software using a 1:1 stoichiometry binding model. Data are the mean K_a and ΔH values ± SEM obtained upon linked-parameter analysis of three independent measurements for each Gads construct.

(fig. S6, right). We envisioned two possible modes of Gads binding to 2pY-LAT: single and paired (Fig. 3A). To ensure the availability of both modes, we applied a sevenfold molar excess of the 2pY-LAT peptide. In the absence of cooperativity, the large molar excess of unbound SH2 binding sites should favor unpaired binding (Fig. 3A, left).

Binding of the monomeric Gads SH2 domain to pY171-LAT resulted in a small shift in Gads mobility, consistent with the added weight of the bound peptide (Fig. 3B, solid and dashed red lines). In contrast, the 2pY-LAT peptide caused a substantial shift toward the dimeric form, suggesting that paired binding was favored (Fig. 3B, red dotted line). Similarly, 2pY-LAT caused a shift from the monomeric form to the dimeric form of full-length Gads, indicating the preferentially paired binding of full-length Gads to LAT (Fig. 3C). The 2pY-LAT–bound SH2 domain dimer was more compact and stable than the spontaneous dimer. Its compact structure was evident by its later elution by size exclusion chromatography (Fig. 3B). To demonstrate its stability, we briefly incubated spontaneous Gads SH2 domain dimers at 37°C to induce monomerization; upon subsequent addition of the 2pY-LAT peptide at 37°C, a stable, induced dimer was formed (Fig. 3D).

Dimerization-dependent discrimination between single- and dual-pLAT

Within the cell, Gads dimerization may promote its preferential binding to dual-pLAT molecules. To test this idea, we performed competitive binding experiments in which the monomeric Gads SH2 domain was incubated with a mixture of 2pY-LAT and pY171-LAT peptides (Fig. 4A). The proportion of Gads molecules that were bound in single or paired configuration was distinguished by their mobility by size exclusion chromatography. Dimerization of the Gads SH2 domain in the presence of the 2pY-LAT peptide was moderately inhibited by the inclusion of a twofold greater concentration of pY171-LAT competitor peptide; nevertheless, >65% of WT Gads SH2 domains remained in the paired binding mode (Fig. 4B, left). This type of preferentially paired binding was observed over a wide range of pY171-LAT competitor concentrations (Fig. 4C, blue curve), with >50% of WT Gads SH2 domains exhibiting paired binding, even at a fourfold excess of competitor peptide. Full-length WT Gads showed an even stronger preference for paired binding (Fig. 4D, left). Together, these results indicate an intrinsic ability of the Gads SH2 domain to discriminate between single- and dual-pLAT molecules by selectively binding to the latter in a paired configuration.

Compared to that of the WT SH2 domain, paired binding of the F92D mutant Gads SH2 domain to 2pY-LAT was more easily disrupted by competing pY171-LAT (Fig. 4B, right). At each concentration of competitor peptide, the extent of 2pY-LAT–induced dimerization of the F92D mutant Gads SH2 domain was less than that of the WT Gads SH2 domain (Fig. 4C). Moreover, the F92D and F92A,R109A mutations substantially impaired the 2pY-LAT–induced dimerization of full-length Gads as well as its discrimination between dual- and single-pLAT (Fig. 4D, center and right). Together, these results suggest that the selectivity of the Gads SH2 domain for dual-pLAT depends on its dimerization

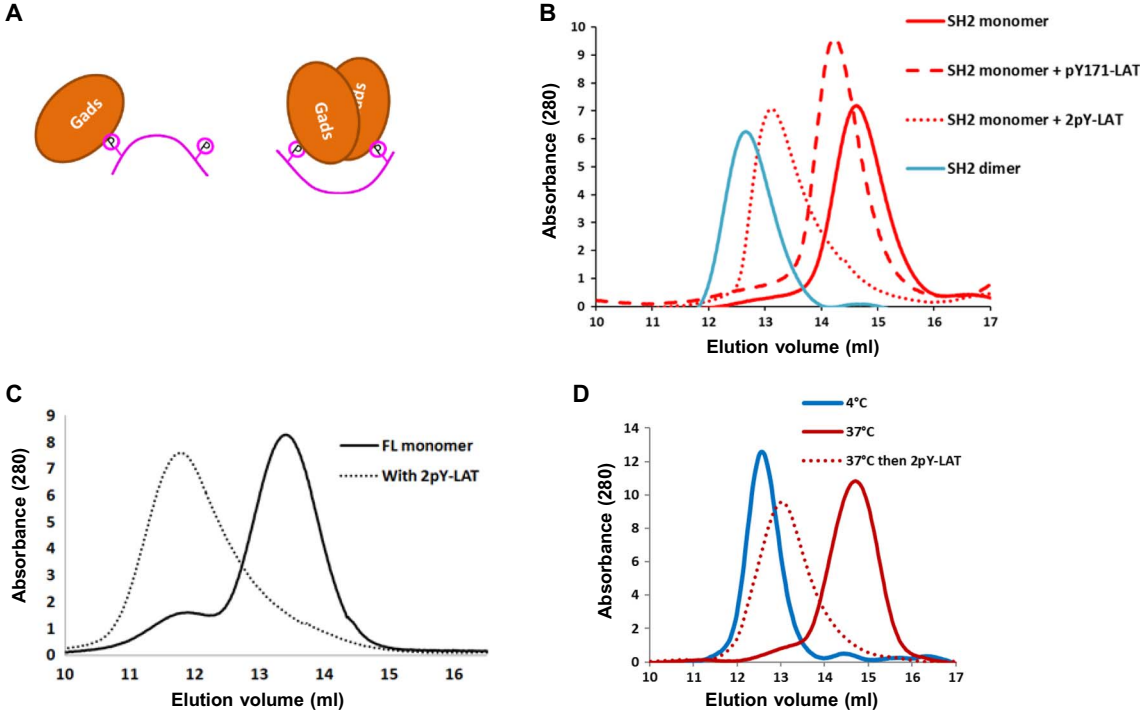

Fig. 3. Preferentially paired binding of the Gads SH2 domain to its dual target sites on LAT. (**A**) The two possible modes of Gads binding to 2pY-LAT. (**B**) Altered fast protein liquid chromatography (FPLC) mobility of the Gads SH2 domain upon binding to single- or dual-pLAT peptides. MBP-Gads SH2 domain (0.7 μM) from the monomeric (red) or dimeric (blue) fraction was incubated on ice for 15 min alone (solid line) or in the presence of 5 μM pY171-LAT (dashed line) or 2pY-LAT (dotted line) peptides before being resolved by size exclusion chromatography. Data are representative of at least five independent experiments. (**C**) Full-length MBP-Gads protein (0.7 μM) from the monomeric fraction was incubated for 15 min at 37°C either alone (solid line) or in the presence of 5 μM 2pY-LAT peptide (dotted line) before being resolved by size exclusion chromatography. Data are representative of three independent experiments. (**D**) Stabilization of the dimeric form of the Gads SH2 domain upon binding to LAT. MBP-Gads SH2 domain (20 μM) from the dimeric fraction was incubated for 30 min on ice (blue) or at 37°C for 15 min (red, solid line), followed by an additional 15 min at 37°C in the presence of 40 μM 2pY-LAT (red, dotted line) before undergoing size exclusion chromatography. Data are representative of three independent experiments.

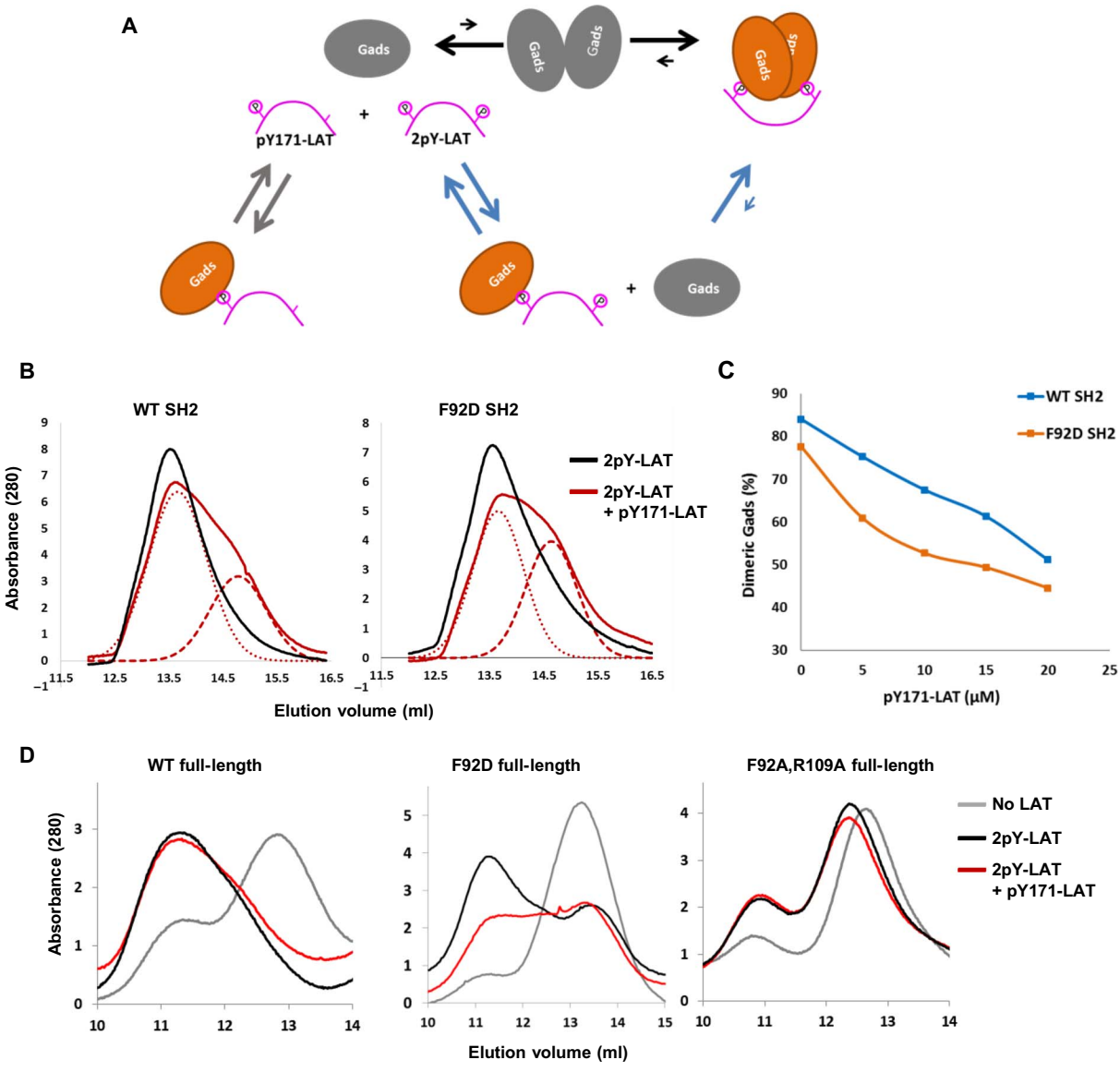

Fig. 4. Gads dimerization interface supports discrimination between single- and dual-pLAT. (**A**) Modes of Gads binding to competing LAT peptides, 2pY-LAT and pY171-LAT. Paired binding to 2pY-LAT can proceed sequentially (blue arrows) or by capture of transient Gads dimers (black arrows). Positive cooperativity occurs if the second Gads molecule binds with higher affinity than the first, resulting in preferentially paired binding. (**B**) Purified monomeric MBP-Gads SH2 (0.7 μM), either WT or F92D, was incubated for 10 min at 37°C with 2pY-LAT (5 μM), in the absence (black) or presence (solid red) of pY171-LAT competitor peptide (10 μM), and resolved by size exclusion chromatography. The red curve was deconvoluted into its constituent dimeric (dotted red) and monomeric (dashed red) components, using the Solve Excel plugin. Data are representative of three independent experiments. (**C**) Competitive binding experiments were performed in triplicate and analyzed as in (B) using the indicated concentrations of competing pY171-LAT. Data are the average percentage of Gads protein found in the dimeric fraction. Standard deviations were too small to depict. The *P* values for all F92D data points, compared to the wild type, were $<10^{-8}$. (**D**) Purified monomeric full-length MBP-Gads (2.5 μM, gray), WT, F92D, or F92A,R109A, was incubated for 10 min at 37°C with 2pY-LAT (25 μM), in the absence (black) or presence (red) of pY171-LAT competitor (50 μM). Data are representative of three independent experiments.

interface, which is required to support the paired binding of full-length Gads to LAT. The preferentially paired binding of the Gads SH2 domain to LAT suggests positive cooperativity, which may result from increased affinity of Gads for a second binding site, once the first site is bound (*39*). Alternatively, cooperativity may reflect the formation of a multimolecular complex (*39*) in which transient Gads dimers bind to LAT at an overall affinity that is greater than the product of the individual site-specific binding constants (*40*). Both mechanisms (Fig. 4A) result in an overrepresentation of paired binding events, relative to the predicted equilibrium binding, which would be expected for independent binding sites. The fold increase in affinity caused by cooperativity can be described as a ratio of the site-specific binding constants for the first and second binding events (*40*). To test whether cooperativity occurred, we generated a mathematical model based on equilibrium binding equations (see the Supplementary Materials). By solving the mathematical model analytically (using the data from Fig. 4C), we calculated the affinity of the second sequential binding event (K_d2) for the WT and F92D mutant Gads SH2 domains (Table 1). The calculated K_d for the K_d2 suggests

a nearly sixfold higher affinity of the second sequential binding event for the WT Gads SH2 domain as compared to the F92D mutant Gads SH2 domain. As one way to estimate the cooperativity, we calculated the fold increase in site-specific binding affinity for the second binding event as compared to the affinity of the binding of Gads to $pTyr^{171}$ (K_d3/K_d2). This ratio was 187-fold for the WT Gads SH2 domain, whereas it was only 87-fold for the F92D mutant, which is consistent with the reduced tendency of the F92D mutant Gads SH2 domain to form LAT-induced dimers and its reduced ability to discriminate between single- and dual-pLAT peptides.

Dependence of TCR signaling on the SH2 dimerization interface of Gads

We next explored the importance of Gads dimerization in intact T cells. We reconstituted dG32 cells, a Jurkat cell–derived, Gads-deficient T cell line (*21*), with N-terminally twin-strep–tagged, green fluorescent protein (GFP)–fused, full-length Gads, either WT, F92D, or F92A,R109A, and then isolated a wide range of GFP^+ cells by sorting (Fig. 5A, left). As previously demonstrated (*21*), the TCR-stimulated increase in the amount of cell surface CD69 correlated with the amount of WT Gads but remained low for GFP-expressing cells. Cells reconstituted with the greatest amounts of the F92D or F92A,R109A Gads SH2 domain mutants responded similarly to Gads-deficient cells (Fig. 5A, right), suggesting that the SH2 dimerization interface was required for Gads-dependent signaling in response to TCR stimulation.

Next, dG32 cells reconstituted with the various Gads-GFP proteins were sorted to isolate cells with equal and homogeneous GFP abundance, and TCR-stimulated molecular interactions and Gads-proximal signaling events were then assessed. Mutation of the SH2 dimerization interface (in either the F92D or F92A,R109A mutants) specifically abolished the TCR-stimulated association of Gads with pLAT without affecting LAT phosphorylation or the constitutive interaction of Gads with SLP-76 (Fig. 5B). Consistent with the impaired formation of the LAT signalosome, TCR-stimulated phosphorylation of PLC-γ1 was markedly impaired in cells reconstituted with the F92D or F92A,R109A mutant Gads proteins (Fig. 5C). Together, these results suggest that the Gads SH2 domain dimerization interface stabilizes its TCR-stimulated interaction with pLAT to facilitate downstream signaling events.

Dependence of FcεRI signaling on the SH2 domain dimerization interface of Gads

To assess the importance of Gads dimerization in FcεRI signaling, Gads-deficient murine bone marrow cells were retrovirally reconstituted with WT Gads-GFP or F92D Gads-GFP and then subjected to in vitro differentiation into mast cells. Fully differentiated BMMCs (WT, Gads-deficient, or Gads-reconstituted) were sensitized with dinitrophenyl (DNP)–specific IgE, which bound equally to all cell types (fig. S7). FcεRI signaling was initiated by the addition of DNP–human serum albumin (HSA) at 37°C, and we then measured three responses that occur at different time scales: calcium flux, which occurs immediately (Fig. 6A); degranulation, which occurs in the first 15 min (Fig. 6B and fig. S8); and secretion of the cytokine interleukin-6 (IL-6), which occurs over a few hours (Fig. 6C).

FACS-based assays revealed binary BMMC responses in all three assays, with the Gads-deficient cells responding at a lower rate compared to WT cells (Fig. 6, A to C; left). Compared to WT BMMCs, the proportion of Gads-deficient BMMCs that exhibited intracellular calcium mobilization was most markedly reduced at the lowest concentrations of DNP-HSA (Fig. 6A, right). Increased intracellular calcium concentrations stimulate degranulation, which results in cell surface expression of CD63 and CD107a (*23*, *41*). The surface abundance of CD63 was reduced in Gads-deficient cells compared to WT cells for all concentrations of DNP-HSA (Fig. 6B, right). Finally, the proportion of Gads-deficient cells that secreted IL-6 in response to FcεRI stimulation was less than that of WT BMMCs for all concentrations of DNP-HSA (Fig. 6C, right).

The extent of the degranulation response in BMMCs reconstituted with WT Gads was dependent on their abundance of Gads-GFP (Fig. 6B, middle, and fig. S8). We therefore analyzed all responses while gating on a narrow window of Gads-GFP abundance. Gads-deficient BMMCs reconstituted with WT Gads-GFP responded similarly to WT BMMCs in all three assays, whereas those reconstituted with the F92D mutant Gads-GFP protein responded similarly to Gads-deficient BMMCs (Fig. 6, A to C, right). Together, these data suggest that the F92D mutation, which prevents spontaneous dimerization of the Gads SH2 domain, completely abrogates Gads-dependent signaling events, both in T cells and in mast cells.

DISCUSSION

The LAT-nucleated signaling complex, which is required for antigen receptor signaling in T cells and mast cells, is a particular example of SH2 domain–mediated multimolecular assembly. The requirement for multiple LAT pYxN motifs to bind Gads or Grb2 is suggestive of cooperativity (*5*, *8*); however, the underlying molecular mechanisms were not known. Here, we describe an SH2 domain–intrinsic mechanism of

Table 1. Binding parameters from the mathematical model of the binding of the Gads SH2 domain to 2pY-LAT. The indicated parameters were calculated from a mathematical model, based on standard equilibrium binding equations, as described in the Supplementary Materials.

	Binding constant at $pTyr^{171}$ (K_d3) (nM)	First sequential constant for binding of a single Gads at either site ($K_d1 = 0.5 \times K_d3$) (nM)	Second sequential binding constant (K_d2) (nM)	Fold increase in site-specific binding affinity at second binding event due to cooperativity (K_d3/K_d2)
WT SH2	177	88.5	0.95	186.5
F92D SH2	472	236	5.4	86.7
Source	Set equal to $pTyr^{171}$ dissociation constant from Fig. 2E	On the basis of an assumption of equivalence of the two binding sites	Calculated from mathematical model of competitive binding data from Fig. 4C	

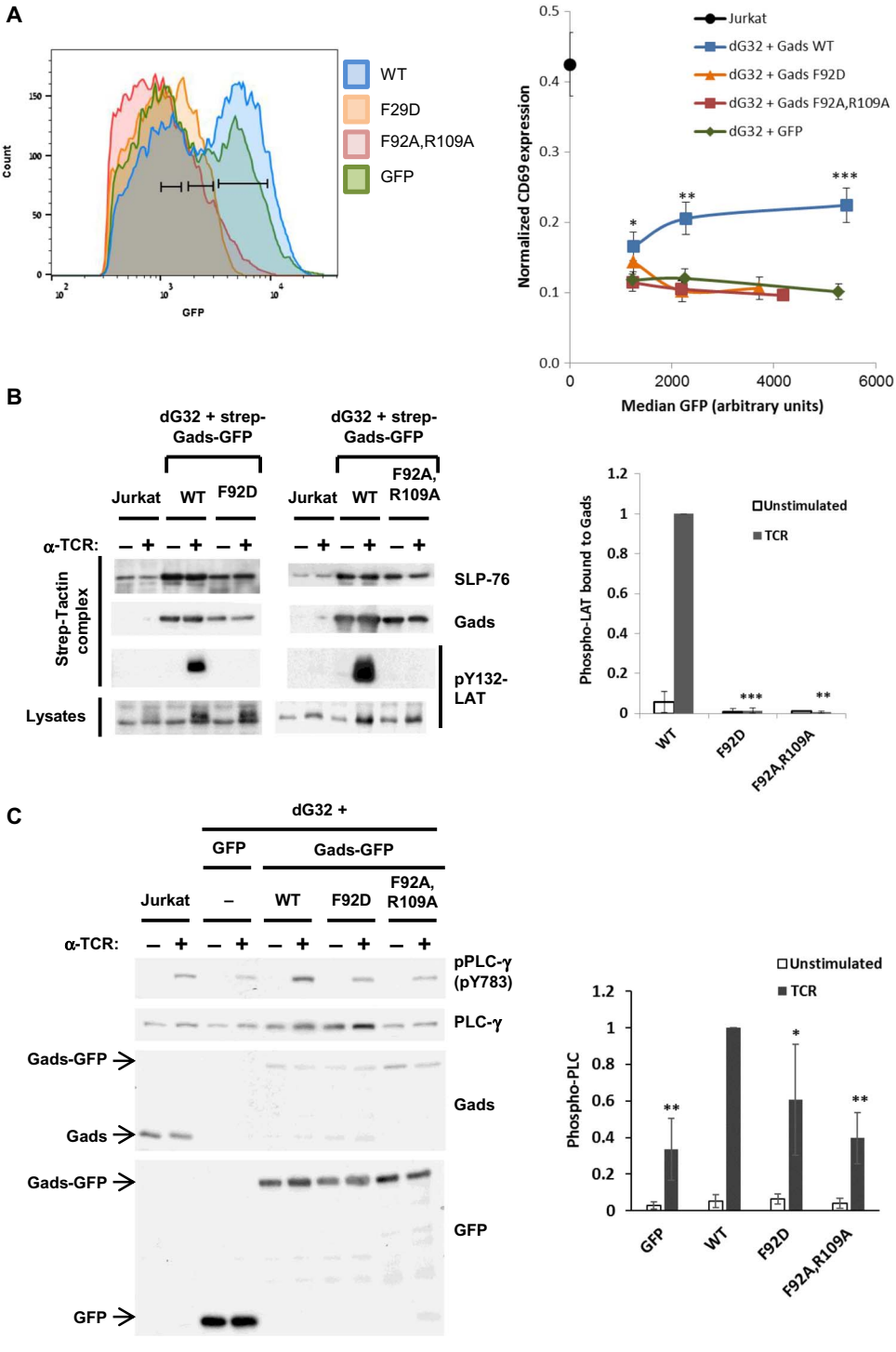

Fig. 5. Gads dimerization is required for TCR signaling. (**A** to **C**) dG32 cells were stably transduced with viruses expressing GFP or the indicated alleles of twin-strep–tagged Gads-GFP, and cells within a broad (A) or narrow, homogeneous range of GFP (B and C) were isolated by fluorescence-activated cell sorting (FACS). (A) CellTrace Violet–barcoded cells were stimulated in quadruplicate overnight with anti-TCR or phorbol 12-myristate 13-acetate (PMA) and then stained with anti-CD69. Median TCR-induced CD69 cell surface abundance was normalized to that induced by PMA within each of the GFP ranges shown at the left. Data are representative of four independent experiments. (B and C) Cells were stimulated for 1 min with anti-TCR (C305) or mock-stimulated and lysed. (B) Strep-Tactin beads were used to purify twin-strep–tagged Gads from the lysates of 60×10^6 cells, and associated SLP-76 and $pTyr^{132}$-pLAT were detected by Western blotting analysis. Right: The ratio of the abundance of pLAT to that of Gads from two (F92A,R109A), three (F92D), or four (WT) experiments, normalized to that of TCR-stimulated WT cells from the same experiment. (C) Cell lysates were analyzed by Western blotting with the indicated antibodies. Right: The intensity of the band corresponding to phosphorylated PLC from four (F92A,R109A and vector), seven (F92D), or eight (WT) experiments, normalized to that of TCR-stimulated WT cells from the same experiment. In all panels, error bars indicate SD. The *P* values were determined for the comparison of TCR-stimulated cells to TCR-stimulated vector (A) or WT-reconstituted cells (B and C). $*P < 0.05$, $**P < 0.005$, $***P < 0.0005$.

cooperativity based on Gads dimerization, which promotes discrimination between dual- and single-pLAT molecules. This selectivity depended on an intact SH2 domain dimerization interface, which was also required for Gads-dependent signaling in cells. Spontaneous dimerization of the Gads SH2 domain was mediated by readily reversible, noncovalent interactions; however, full-length Gads dimers exhibited increased stability at a physiologic temperature, compared to the isolated SH2 domain. On the basis of molecular modeling, we designed SH2 domain point mutations, F92D and F92A,R109A, which specifically disrupted spontaneous Gads dimerization but only moderately affected the affinity of the mutant Gads proteins for the single-pLAT peptide. Inducible Gads dimerization was observed upon paired binding of Gads to dual-pLAT. The inducible dimer was more compact than those formed spontaneously, as well as being more stable at 37°C, which is consistent with its potential to play a physiologically relevant role in intact cells.

The marked overrepresentation of paired binding events in our experiments provides evidence for SH2 domain–intrinsic cooperativity, which was captured by mathematical modeling as an increase in binding affinity upon binding of a second Gads molecule to 2pY-LAT. This increase in binding affinity was 2.2-fold higher for the WT Gads SH2 domain than for the F92D mutant. The difference suggests that cooperativity, in part, may reflect the capture and stabilization of transient Gads dimers upon binding to 2pY-LAT. In the absence of direct structural information, we speculate that transient dimerization of the Gads SH2 domain may generate an additional binding interface outside

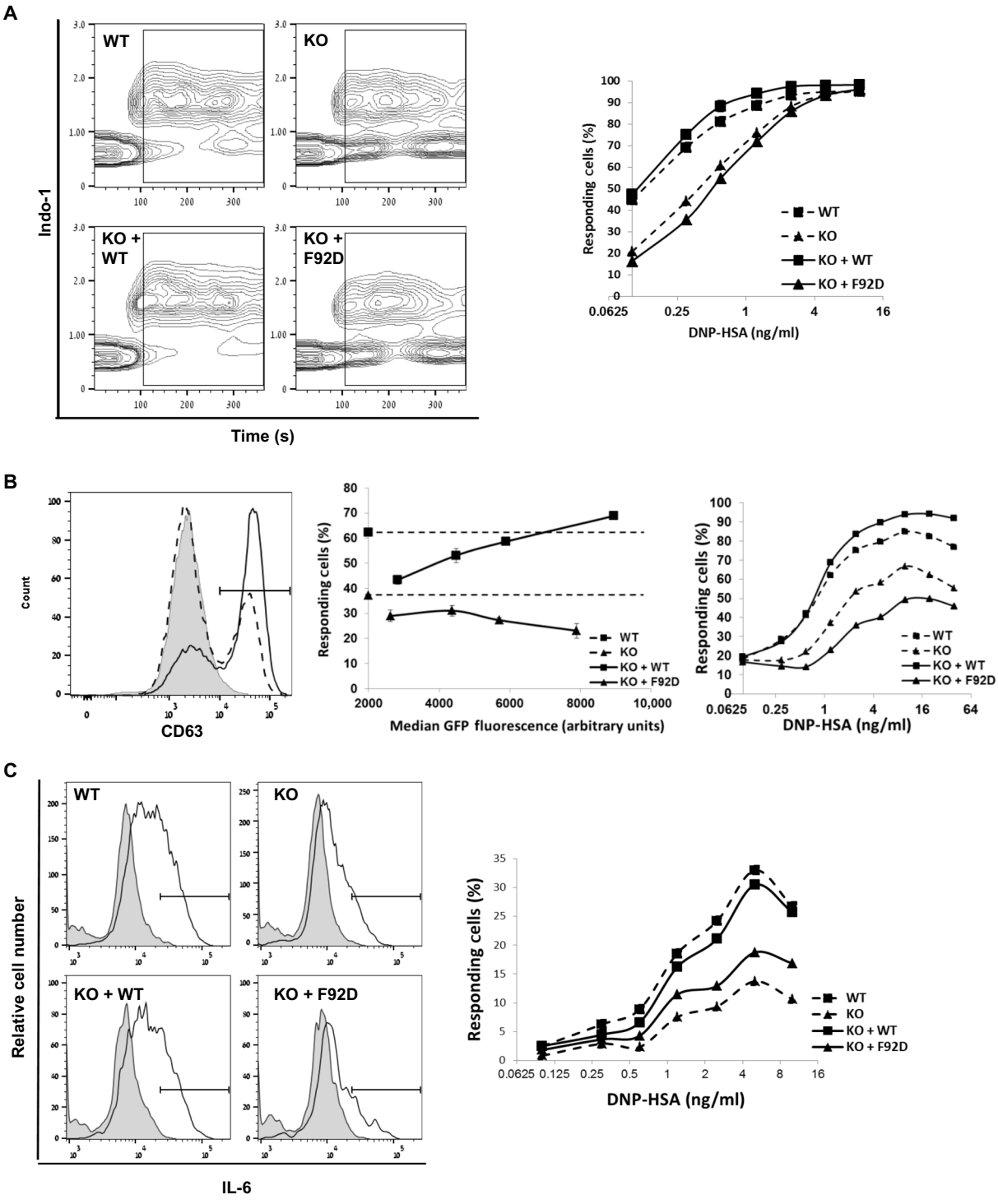

Fig. 6. F92D mutation disrupts FcεRI signaling. (**A** to **C**) Fully differentiated BMMCs, derived from wild type (WT), Gads-deficient [knockout (KO)], or retrovirally reconstituted KO bone marrow cells (KO + WT or KO + F92D), were barcoded, sensitized with IgE (anti-DNP), and stimulated at 37°C with DNP-HSA. Responses were analyzed by FACS while gating on matched, narrow regions of Gads-GFP. (A) Left: Changes in intracellular calcium, with DNP-HSA (0.6 ng/ml) added at 60 s. Cells above the baseline during the last 200 s were considered to be responsive. Right: Percentage of responding cells as a function of stimulant concentration. Data are representative of three independent experiments. (B) Left: BMMCs were left unstimulated (filled histogram) or stimulated for 15 min with DNP-HSA (1.2 ng/ml, solid line, WT; dashed line, F92D) and then fixed and stained with anti–CD63-PE. The indicated gate defined the $CD63^+$ responding cells. Middle: $CD63^+$ responding cells, as a function of Gads-GFP abundance (data are the average of triplicate measurements; error bars indicate SD; dotted lines indicate the response of WT and KO cells in the same experiment). Right: $CD63^+$ responding cells as a function of stimulant concentration. Data are representative of five independent experiments. (C) Left: Cells were unstimulated (filled histograms) or stimulated for 4.5 hours with DNP-HSA (0.6 ng/ml, black line), and the $IL\text{-}6^+$ responding cells, defined by the indicated gate, were identified by intracellular staining. Right: $IL\text{-}6^+$ responding cells, as a function of stimulant concentration. Data are representative of two independent experiments.

the pTyr binding pocket, which supports the high-affinity binding of Gads to dual-pLAT, perhaps by interacting with the conserved LAT sequence spanning from $pTyr^{171}$ to $pTyr^{191}$.

A distinct mechanism of SH2 domain dimerization, which involves α helix swapping, was observed in structural studies of the Grb2, Nck, and Itk SH2 domains (*42*–*44*) but not in published structures of the Gads SH2 domain. Swapping of Grb2 α helices markedly decreases the affinity of Grb2 for pTyr-containing peptides (*45*). An additional mechanism of Grb2 dimerization through SH2-SH3 domain interactions was reported but is inconsistent with binding to pTyr-containing peptides (*46*). In contrast, Gads SH2 domain dimerization increased the affinity and selectivity of paired binding to 2pY-LAT, suggesting that this constitutes a previously uncharacterized SH2 domain–intrinsic mechanism of cooperativity. In the context of full-length Gads, the F92D and F92A,R109A mutations markedly reduced its ability to discriminate between dual- and single-pLAT molecules and abrogated Gads-dependent signaling in T cells and BMMCs. This phenotype was most apparent in BMMCs under conditions of weak antigenic stimulation. Under these conditions, incompletely phosphorylated LAT molecules may predominate, and Gads dimerization may be required to prioritize complex formation at fully phosphorylated LAT molecules. In some assays, cells reconstituted with the F92D mutant Gads protein exhibited a decreased response compared to that of Gads-deficient cells, which suggests that by abrogating Gads dimerization, we may have unmasked a negative signaling function of Gads.

We also consider the possibility that Gads dimerization may affect downstream signaling through additional mechanisms. The competition of Gads and Grb2 for their shared binding sites on LAT may be influenced by Gads dimerization, thereby altering the balance between the Gads–SLP-76 and Grb2-SOS signaling pathways. In addition, paired binding of Gads to LAT may restructure the LAT molecule in a way that enables its binding to additional signaling molecules. Consistent with this notion, mutation of the Gads binding sites on LAT decreases its binding to PLC-γ1 (*5*, *7*, *8*). Finally, the F92D mutation, by placing a strong negative charge within the dimerization interface of the Gads SH2 domain, may disrupt dimerization of the associated SLP-76 (*47*, *48*), thereby affecting the overall structure of the SLP-76 nucleated complex. These and other possibilities require further study.

MATERIALS AND METHODS

Plasmids

For the expression of recombinant MBP-tagged Gads, the complementary DNA (cDNA) encoding human Gads was subcloned into the Bam HI and Eco RI sites of pMAL-C5x (New England Biolabs). Deletion mutants were derived by polymerase chain reaction (PCR) amplification of the entire plasmid using Phusion Hot Start Flex DNA Polymerase (New England Biolabs) and 5′-phosphorylated primers that bordered the deleted area on both sides. The resulting PCR products were circularized with Fast-Link Ligase (Epicentre). Mutant MBP-Gads constructs were as follows (deleted residues in parentheses): ΔN-SH3 Gads (2 to 53), ΔC-SH3 Gads (274 to 328), ΔC-SH3 + linker (154 to 328), and SH2 domain only (2 to 53 and 154 to 330). His-tagged constructs were generated by replacing the MBP reading frame with an N-terminal 6-His tag. For retroviral infections, the cDNA encoding full-length Gads with an N-terminal twin-strep tag (*49*) was subcloned into the pMIGR vector, which contains an internal ribosomal entry site (IRES)–GFP cassette (*50*). We incorporated the A206K GFP mutation to prevent GFP dimerization (*51*) and used a phusion-based strategy to remove the IRES sequence and fuse the C terminus of Gads with monomeric GFP, thus generating a single open reading frame encoding Gads that is N-terminally tagged with a twin-strep tag and C-terminally tagged with monomeric GFP. Point mutations in Gads were generated by QuikChange. All constructs were verified by sequencing the entire open reading frame.

Antibodies

The monoclonal antibody C305 was used to stimulate Jurkat cell–derived cell lines through the TCR (*52*). Phycoerythrin (PE)/Cy5-conjugated anti-human CD69, anti-CD16/32, PE-conjugated anti-mouse CD63, allophycocyanin (APC)–conjugated anti-mouse CD107a, and APC-conjugated rat immunoglobulin G2b (isotype control) antibodies were from BioLegend. Rabbit anti-Gads and rabbit anti–PLC-γ1 antibodies were from Santa Cruz Biotechnology. Anti-pLAT (pY132) antibody was from BioSource. Rabbit anti-GFP antibody was a gift from A. Stanhill (Sheba Hospital and Tikcro Technologies). Anti–pPLC-γ1 (pY783) was from MBL International. Anti-DNP IgE was from Sigma-Aldrich. PE-conjugated anti-IgE antibody was from SouthernBiotech. APC-conjugated anti-mouse CD117 (cKit) was from BioGems. PerCP-eFluor710–conjugated anti-mouse IL-6 antibody was from eBioscience.

Production and purification of recombinant proteins

Escherichia coli strain BL21-CodonPlus (Agilent Technologies) expressing MBP- or His-tagged Gads proteins was grown in an autoinduction medium (*53*) containing carbenicillin (5 μg/ml) and chloramphenicol (25 μg/ml) at 37°C for 4 hours and then were shifted to 18°C for 16 hours. Cells were harvested by centrifugation at 8000*g* for 50 min at 4°C and then were resuspended in column buffer [20 mM Hepes (pH 7.3), 100 mM NaCl, 1 mM EDTA, and 10% glycerol] for MBP-tagged proteins or binding buffer [20 mM Hepes (pH 7.3), 200 mM NaCl, and 20 mM imidazole] for His-tagged proteins, with protease inhibitors and deoxyribonuclease added before cell disruption by EmulsiFlex-C3 (Avestin). All purification steps were conducted at 4°C. Lysates were centrifuged at 10,000*g* for 50 min, and the supernatant was applied onto a preequilibrated, 2.5-cm diameter, 4-ml bed volume gravity column (Econo-Column, Bio-Rad). MBP proteins were incubated with amylose resin (New England Biolabs) for 2 hours and then were washed three times and eluted for 2 hours in column buffer supplemented with 10 mM maltose. His-tagged proteins were incubated with Ni-NTA His-Bind Resin (Qiagen) for 2 hours and then were washed with binding buffer and eluted in binding buffer containing 300 mM imidazole. Eluted proteins were collected and concentrated with an Amicon Ultra-15 Centrifugal Filter Unit, with a 30-kDa molecular weight cutoff for MBP-tagged proteins and a 3-kDa molecular weight cutoff for His-tagged proteins.

Fast protein liquid chromatography

MBP- and His-tagged proteins were resolved by size exclusion chromatography at 12°C using an AKTA FPLC system (GE Healthcare) fitted with Superdex 200 10/300 or 16/60 HiLoad for MBP-tagged proteins and Superdex 75 10/300 for His-tagged proteins in column buffer containing 20 mM Hepes (pH 7.3), 100 mM NaCl, 1 mM EDTA, and 10% glycerol.

Isothermal titration calorimetry

Isothermal titration calorimetry (ITC) was carried out at 25°C on a MicroCal 200 titration microcalorimeter (GE Healthcare), with all

components resuspended or purified in column buffer. Aliquots (2 μl) of 0.2 mM pY171-LAT peptide were injected from a rotating syringe at 800 rpm into a sample cell containing 234 μl of 0.02 mM MBP-Gads SH2. The duration of each injection was 4 s, whereas the delay between injections was 180 s. Data analysis was performed with AFFINImeter software.

Peptides

LAT peptides were synthesized and purified by GL Biochem or Pepmic Co. Ltd., validated by mass spectrometry and high-performance liquid chromatography analysis, and resuspended in column buffer. Peptides were 29 residues long, were of the sequence DDYVNVPESGESAEASLDGSREYVNVSQE, encompassing LAT residues Tyr^{171} and Tyr^{191}, and were either doubly phosphorylated (2pY-LAT) or singly phosphorylated on Tyr^{171} (pY171-LAT). To determine the concentration of the pY171-LAT peptide, we measured its binding to purified Gads SH2 domain by ITC and adjusted the peptide concentration to reflect a 1:1 stoichiometry. The concentration of the 2pY-LAT peptide was also determined by ITC by measuring its ability to sequester Gads SH2 domains and prevent their binding to the pY171-LAT peptide.

Thermal stability measurement

Nano-DSF was performed with the Prometheus NT.48 instrument (NanoTemper Technologies) to detect the shift in intrinsic tryptophan fluorescence that occurs upon protein denaturation (*35*). This instrument is also equipped with a light-scattering detector to measure the onset of protein aggregation. Purified recombinant Gads protein (20 μM) was loaded into nano-DSF–grade standard capillaries, and the temperature was increased at a rate of 1°C/min from 15° to 95°C while measuring the ratio of tryptophan fluorescence emission intensity (350/330), as described previously (*35*). Data were analyzed with NanoTemper software.

Size exclusion chromatography and multiangle light scattering

The average molecular weights of Gads proteins were determined by SEC-MALS. The system consisted of an ÄKTA avant 25 coupled to an ultraviolet detector (GE Healthcare) and a miniDAWN triple-angle light-scattering detector (Wyatt Technology). MBP-tagged Gads protein (300 μg), either full-length or SH2 domain alone, was loaded into a Superdex 200 10/300 column (GE Healthcare) and eluted at 0.5 ml/min with column buffer [20 mM Hepes (pH 7.3), 100 mM NaCl, 1 mM EDTA, and 10% glycerol]. Data collection and analysis were performed with Wyatt's ASTRA 6.1.1 software.

Ras recruitment system

Yeast growth, transfection, and functional screening for bait-prey interactions with the RRS were conducted as previously described (*54*). The Gads RRS bait was designed by cloning the cDNA encoding full-length Gads into pMet-myc-Ras (*54*), where it was fused in frame to the 3′ end of the Ras protein open reading frame. The Gads prey was designed by subcloning the cDNA encoding full-length Gads into pMyr (*55*) in frame with an N-terminal myristoylation sequence. CDC25-2 temperature-sensitive yeast cells were transfected with the Ras-Bait and Myristoylated-Prey plasmids. Transformants were selected at the permissive temperature (25°C) and subsequently replica-plated onto appropriate medium and grown at the restrictive temperature (36°C). In this system, growth at 36°C indicates an interaction between the bait and prey proteins.

Cell lines

The Gads-deficient, Jurkat cell–derived T cell line dG32 was previously described (*21*). Cells were retrovirally reconstituted with N-terminally twin-strep–tagged Gads-GFP and then sorted by FACS for cells with similar amounts of GFP.

Cell stimulation and lysis

Jurkat- and dG32-derived T cell lines were stimulated for 1 min at 37°C with anti-TCR antibody (C305) and then were lysed at 10^8 cells/ml in ice-cold lysis buffer [20 mM Hepes (pH 7.3), 1% Triton X-100, 150 mM NaCl, 10% glycerol, 10 mM NaF, 1 mM Na_3VO_4, aprotinin (10 μg/ml), 2 mM EGTA, leupeptin (10 μg/ml), 2 mM phenylmethanesulfonyl fluoride, pepstatin (1 μg/ml), and 1 mM dithiothreitol]. For immunoprecipitation experiments, lysis buffer was supplemented with 0.1% *n*-dodecyl-β-D-maltoside (Calbiochem).

Strep-Tactin bead purification of twin-strep–tagged Gads

Cell lysates were centrifuged twice at 16,000*g* for 10 min at 4°C, and twin-strep–tagged Gads-GFP was affinity-purified by tumbling end-over-end for 30 min at 4°C with Strep-Tactin Superflow high capacity beads (IBA), using about 7 μl of bead suspension for every 20 million cells lysed. After three rapid washes with cold lysis buffer, the isolated complexes were analyzed by Western blotting. Western blots were developed with EZ-ECL reagent (Biological Industries), and bands on scanned films were quantified with TotalLab Quant software.

Barcoding

To decrease experimental variation, we adapted a barcoding approach (*56*) in which cell lines were differentially labeled with fourfold dilutions of CellTrace Violet or CellTrace Far Red (Life Technologies). Phosphate-buffered saline (PBS)–washed cells were incubated with gentle mixing for 20 min in the dark at room temperature in 0.015 to 3.75 μM CellTrace Violet or 0.003 to 0.75 μM CellTrace Far Red in PBS. Staining was stopped by adding four volumes of medium containing 10% fetal calf serum and incubating the samples for an additional 5 min at room temperature. Cells were then washed and mixed together in the same tube before being subjected to stimulation and FACS-based functional assays. Data analysis was performed while gating on the differentially barcoded populations within the sample. In all cases, controls were performed to verify that the barcoding reaction had no effect on cellular responsiveness.

T cell activation

TCR-stimulated increases in CD69 abundance were measured essentially as described previously (*21*), except that cells were barcoded with CellTrace Violet and mixed together before being stimulated. Median TCR-stimulated CD69 cell surface expression was normalized to the median PMA-stimulated cell surface expression of CD69 within the same cell population gate.

Mice

Gads-deficient mice (*28*) on the Balb/c genetic background were provided by C. J. McGlade (University of Toronto). WT Balb/c mice were purchased from Harlan. Mice were maintained under specific pathogen–free conditions under veterinary supervision in accordance with the guidelines of our Institutional Animal Ethics Committee.

Generation of BMMCs

Bone marrow cells were obtained from the femurs and tibias of WT or Gads-deficient mice and were cultured in mast cell medium [Iscove's

modified Dulbecco's medium, supplemented with 16% iron-fortified bovine calf serum, penicillin (100 U/ml), streptomycin (100 μg/ml), glutamine (2 mg/ml), 50 μM 2-mercaptoethanol, 1 mM sodium pyruvate, 1× nonessential amino acids, and 10 mM Hepes] containing IL-3 (10 ng/ml) and stem cell factor (10 ng/ml). Retroviruses encoding different Gads-GFP variants or GFP alone were packaged in Plat-E cells (Cell Biolabs) using Lipofectamine 3000 transfection reagent (Invitrogen). Cells were infected twice, on days 2 and 3 of culturing, and were sorted for GFP^+ cells during the week 4. Experiments were begun when the cells were ≥95% $cKit^+FcεRI^+$, as shown by flow cytometry analysis.

FcεRI signaling assays

Fully differentiated BMMCs were washed in cytokine-free medium, barcoded, and sensitized overnight at 37°C in medium containing IL-3 (10 ng/ml) and anti-DNP IgE (0.1 μg/ml). For Ca^{2+} assays, CellTrace Far Red–barcoded, sensitized BMMCs were washed and incubated for 20 min at 37°C in Tyrode's buffer (*57*) containing 1 mM probenicid (Sigma-Aldrich) and indo-1 AM (3 μg/ml) (eBioscience), diluted 10-fold in 37°C Tyrode's buffer for an additional 20 min, and then washed twice and resuspended at 2×10^6 cells/ml in Tyrode's buffer. Intracellular calcium was measured ratiometrically by flow cytometry at 37°C, over a 5-min time course. After 60 s of baseline measurement, the cells were treated with DNP-HSA (Sigma-Aldrich). CellTrace Violet–barcoded, sensitized BMMCs were used to assess degranulation and IL-6 production. For degranulation assays, cells were stimulated with DNP-HSA in Tyrode's buffer for 15 min, fixed with 2% paraformaldehyde for 15 min at room temperature, and stained with PE-conjugated anti-CD63 or APC-conjugated anti-CD107a antibodies. IL-6 production was assessed after 4.5 hours of stimulation with DNP-HSA by intracellular staining with IL-6 PerCP-eFluor710, as described previously (*41*).

Computational alanine-scanning of the Gads SH2 domain dimer interface

The predicted structure of the Gads SH2 domain dimer bound to LAT was constructed by superimposition of the crystal structures of the Gads SH2 domain bound to short LAT $pTry^{171}$ (PDB: 1R1P) and to LAT $pTyr^{191}$ (PDB: 1R1Q) peptides (*37*). The modeled structure of the Gads SH2 domain dimer has subunit A bound to LAT $pTyr^{171}$ (PDB: 1R1P) and subunit B bound to LAT $pTyr^{191}$ (PDB: 1R1Q). Computational alanine-scanning of the modeled Gads SH2 domain dimer structure was performed with the Robetta server (*58*, *59*). The positive changes in binding free energy $\Delta\Delta G_{bind} > 0$ indicate destabilization of the dimer interface upon mutation to alanine.

Statistical analysis

Statistical analysis was performed with the two-tailed Student's *t* test.

SUPPLEMENTARY MATERIALS

www.sciencesignaling.org/cgi/content/full/10/498/eaal1482/DC1

Mathematical modeling

Fig. S1. Molecular weights of the monomeric and dimeric forms of Gads.

Fig. S2. Thermal stabilities of the monomeric and dimeric forms of MBP-Gads SH2.

Fig. S3. Model of the SH2 domain dimerization interface.

Fig. S4. The R109D, R109A, and F92A single mutations are not sufficient to disrupt Gads SH2 dimerization.

Fig. S5. Thermal stabilities of nondimerizing Gads mutants.

Fig. S6. Multiple sequence alignment of the C-terminal regions of LAT molecules from 15 mammalian species.

Fig. S7. Cell surface FcεRI abundance is independent of Gads.

Fig. S8. FcεRI-induced cell surface expression of the degranulation marker CD107a depends on the Gads dimerization interface.

Table S1. Summary of the abbreviations used in the mathematical model.

Table S2. Calculated kinetic constants.

References (*60*)

REFERENCES AND NOTES

1. T. Kambayashi, G. A. Koretzky, Proximal signaling events in FcεRI-mediated mast cell activation. *J. Allergy Clin. Immunol.* **119**, 544–552 (2007).
2. R. J. Brownlie, R. Zamoyska, T cell receptor signalling networks: Branched, diversified and bounded. *Nat. Rev. Immunol.* **13**, 257–269 (2013).
3. A. K. Chakraborty, A. Weiss, Insights into the initiation of TCR signaling. *Nat. Immunol.* **15**, 798–807 (2014).
4. J. C. D. Houtman, R. A. Houghtling, M. Barda-Saad, Y. Toda, L. E. Samelson, Early phosphorylation kinetics of proteins involved in proximal TCR-mediated signaling pathways. *J. Immunol.* **175**, 2449–2458 (2005).
5. J. Lin, A. Weiss, Identification of the minimal tyrosine residues required for linker for activation of T cell function. *J. Biol. Chem.* **276**, 29588–29595 (2001).
6. P. E. Paz, S. Wang, H. Clarke, X. Lu, D. Stokoe, A. Abo, Mapping the Zap-70 phosphorylation sites on LAT (linker for activation of T cells) required for recruitment and activation of signalling proteins in T cells. *Biochem. J.* **356**, 461–471 (2001).
7. W. Zhang, R. P. Trible, M. Zhu, S. K. Liu, C. J. McGlade, L. E. Samelson, Association of Grb2, Gads and phospholipase C-γ1 with phosphorylated LAT tyrosine residues. Effect of LAT tyrosine mutations on t cell antigen receptor-mediated signaling. *J. Biol. Chem.* **275**, 23355–23361 (2000).
8. M. Zhu, E. Janssen, W. Zhang, Minimal requirement of tyrosine residues of linker for activation of T cells in TCR signaling and thymocyte development. *J. Immunol.* **170**, 325–333 (2003).
9. I. K. Jang, J. Zhang, H. Gu, Grb2, a simple adapter with complex roles in lymphocyte development, function, and signaling. *Immunol. Rev.* **232**, 150–159 (2009).
10. S. K.-W. Liu, D. M. Berry, C. J. McGlade, The role of Gads in hematopoietic cell signalling. *Oncogene* **20**, 6284–6290 (2001).
11. D. M. Berry, P. Nash, S. K.-W. Liu, T. Pawson, C. J. McGlade, A high-affinity Arg-X-X-Lys SH3 binding motif confers specificity for the interaction between Gads and SLP-76 in T cell signaling. *Curr. Biol.* **12**, 1336–1341 (2002).
12. M. Harkiolaki, M. Lewitzky, R. J. C. Gilbert, E. Jones, R. P. Bourette, G. Mouchiroud, H. Sondermann, I. Moarefi, S. M. Feller, Structural basis for SH3 domain-mediated high-affinity binding between Mona/Gads and SLP-76. *EMBO J.* **22**, 2571–2582 (2003).
13. Q. Liu, D. Berry, P. Nash, T. Pawson, C. J. McGlade, S. S.-C. Li, Structural basis for specific binding of the Gads SH3 domain to an RxxK motif-containing SLP-76 peptide: A novel mode of peptide recognition. *Mol. Cell* **11**, 471–481 (2003).
14. Y. Bogin, C. Ainey, D. Beach, D. Yablonski, SLP-76 mediates and maintains activation of the Tec family kinase ITK via the T cell antigen receptor-induced association between SLP-76 and ITK. *Proc. Natl. Acad. Sci. U.S.A.* **104**, 6638–6643 (2007).
15. S. C. Bunnell, M. Diehn, M. B. Yaffe, P. R. Findell, L. C. Cantley, L. J. Berg, Biochemical interactions integrating Itk with the T cell receptor-initiated signaling cascade. *J. Biol. Chem.* **275**, 2219–2230 (2000).
16. M. Sela, Y. Bogin, D. Beach, T. Oellerich, J. Lehne, J. E. Smith-Garvin, M. Okumura, E. Starosvetsky, R. Kosoff, E. Libman, G. Koretzky, T. Kambayashi, H. Urlaub, J. Wienands, J. Chernoff, D. Yablonski, Sequential phosphorylation of SLP-76 at tyrosine 173 is required for activation of T and mast cells. *EMBO J.* **30**, 3160–3172 (2011).
17. S. Devkota, R. E. Joseph, L. Min, D. Bruce Fulton, A. H. Andreotti, Scaffold protein SLP-76 primes PLCγ1 for activation by ITK-mediated phosphorylation. *J. Mol. Biol.* **427**, 2734–2747 (2015).
18. H. Asada, N. Ishii, Y. Sasaki, K. Endo, H. Kasai, N. Tanaka, T. Takeshita, S. Tsuchiya, T. Konno, K. Sugamura, Grf40, a novel Grb2 family member, is involved in T cell signaling through interactions with SLP-76 and LAT. *J. Exp. Med.* **189**, 1383–1390 (1999).
19. C.-L. Law, M. K. Ewings, P. M. Chaudhary, S. A. Solow, T. J. Yun, A. J. Marshall, L. Hood, E. A. Clark, GrpL, a Grb2-related adaptor protein, interacts with SLP-76 to regulate nuclear factor of activated T cell activation. *J. Exp. Med.* **189**, 1243–1253 (1999).
20. S. K. Liu, N. Fang, G. A. Koretzky, C. J. McGlade, The hematopoietic-specific adaptor protein Gads functions in T-cell signaling via interactions with the SLP-76 and LAT adaptors. *Curr. Biol.* **9**, 67–75 (1999).
21. J. Lugassy, J. Corso, D. Beach, T. Petrik, T. Oellerich, H. Urlaub, D. Yablonski, Modulation of TCR responsiveness by the Grb2-family adaptor, Gads. *Cell. Signal.* **27**, 125–134 (2015).
22. S. Saitoh, R. Arudchandran, T. S. Manetz, W. Zhang, C. L. Sommers, P. E. Love, J. Rivera, L. E. Samelson, LAT is essential for FcεRI-mediated mast cell activation. *Immunity* **12**, 525–535 (2000).

23. S. Yamasaki, M. Takase-Utsugi, E. Ishikawa, M. Sakuma, K. Nishida, T. Saito, O. Kanagawa, Selective impairment of FcεRI-mediated allergic reaction in Gads-deficient mice. *Int. Immunol.* **20**, 1289–1297 (2008).
24. V. I. Pivniouk, T. R. Martin, J. M. Lu-Kuo, H. R. Katz, H. C. Oettgen, R. S. Geha, SLP-76 deficiency impairs signaling via the high-affinity IgE receptor in mast cells. *J. Clin. Invest.* **103**, 1737–1743 (1999).
25. J. C. D. Houtman, Y. Higashimoto, N. Dimasi, S. Cho, H. Yamaguchi, B. Bowden, C. Regan, E. L. Malchiodi, R. Mariuzza, P. Schuck, E. Appella, L. E. Samelson, Binding specificity of multiprotein signaling complexes is determined by both cooperative interactions and affinity preferences. *Biochemistry* **43**, 4170–4178 (2004).
26. S. L. Dalheimer, L. Zeng, K. E. Draves, A. Hassaballa, N. N. Jiwa, T. D. Parrish, E. A. Clark, T. M. Yankee, Gads-deficient thymocytes are blocked at the transitional single positive $CD4^+$ stage. *Eur. J. Immunol.* **39**, 1395–1404 (2009).
27. T. M. Yankee, T. J. Yun, K. E. Draves, K. Ganesh, M. J. Bevan, K. Murali-Krishna, E. A. Clark, The Gads (GrpL) adaptor protein regulates T cell homeostasis. *J. Immunol.* **173**, 1711–1720 (2004).
28. J. Yoder, C. Pham, Y.-M. Iizuka, O. Kanagawa, S. K. Liu, J. McGlade, A. M. Cheng, Requirement for the SLP-76 adaptor GADS in T cell development. *Science* **291**, 1987–1991 (2001).
29. J. L. Clements, B. Yang, S. E. Ross-Barta, S. L. Eliason, R. F. Hrstka, R. A. Williamson, G. A. Koretzky, Requirement for the leukocyte-specific adapter protein SLP-76 for normal T cell development. *Science* **281**, 416–419 (1998).
30. V. Pivniouk, E. Tsitsikov, P. Swinton, G. Rathbun, F. W. Alt, R. S. Geha, Impaired viability and profound block in thymocyte development in mice lacking the adaptor protein SLP-76. *Cell* **94**, 229–238 (1998).
31. W. Zhang, C. L. Sommers, D. N. Burshtyn, C. C. Stebbins, J. B. DeJarnette, R. P. Trible, A. Grinberg, H. C. Tsay, H. M. Jacobs, C. M. Kessler, E. O. Long, P. E. Love, L. E. Samelson, Essential role of LAT in T cell development. *Immunity* **10**, 323–332 (1999).
32. T. S. Finco, T. Kadlecek, W. Zhang, L. E. Samelson, A. Weiss, LAT is required for TCR-mediated activation of PLCγ1 and the Ras pathway. *Immunity* **9**, 617–626 (1998).
33. D. Yablonski, M. R. Kuhne, T. Kadlecek, A. Weiss, Uncoupling of nonreceptor tyrosine kinases from PLC-γ1 in an SLP-76-deficient T cell. *Science* **281**, 413–416 (1998).
34. M. Y. Bilal, E. Y. Zhang, B. Dinkel, D. Hardy, T. M. Yankee, J. C. D. Houtman, GADS is required for TCR-mediated calcium influx and cytokine release, but not cellular adhesion, in human T cells. *Cell. Signal.* **27**, 841–850 (2015).
35. D. B. Temel, P. Landsman, M. L. Brader, in *Methods in Enzymology*, L. F. Andrew, Ed. (Academic Press, 2016), vol. 567, pp. 359–389.
36. Y. C. Broder, S. Katz, A. Aronheim, The Ras recruitment system, a novel approach to the study of protein–protein interactions. *Curr. Biol.* **8**, 1121–1124 (1998).
37. S. Cho, C. A. Velikovsky, C. P. Swaminathan, J. C. D. Houtman, L. E. Samelson, R. A. Mariuzza, Structural basis for differential recognition of tyrosine-phosphorylated sites in the linker for activation of T cells (LAT) by the adaptor Gads. *EMBO J.* **23**, 1441–1451 (2004).
38. R. P. Bahadur, P. Chakrabarti, F. Rodier, J. Janin, Dissecting subunit interfaces in homodimeric proteins. *Proteins* **53**, 708–719 (2003).
39. A. Whitty, Cooperativity and biological complexity. *Nat. Chem. Biol.* **4**, 435–439 (2008).
40. E. Freire, A. Schön, A. Velazquez-Campoy, in *Methods in Enzymology*, L. Michael, J. M. H. Johnson, K. A. Gary, Eds. (Academic Press, 2009), vol. 455, pp. 127–155.
41. N. Föger, A. Jenckel, Z. Orinska, K.-H. Lee, A. C. Chan, S. Bulfone-Paus, Differential regulation of mast cell degranulation versus cytokine secretion by the actin regulatory proteins Coronin1a and Coronin1b. *J. Exp. Med.* **208**, 1777–1787 (2011).
42. N. Schiering, E. Casale, P. Caccia, P. Giordano, C. Battistini, Dimer formation through domain swapping in the crystal structure of the Grb2-SH2–Ac-pYVNV complex. *Biochemistry* **39**, 13376–13382 (2000).
43. S. Frese, W.-D. Schubert, A. C. Findeis, T. Marquardt, Y. S. Roske, T. E. B. Stradal, D. W. Heinz, The phosphotyrosine peptide binding specificity of Nck1 and Nck2 Src homology 2 domains. *J. Biol. Chem.* **281**, 18236–18245 (2006).
44. R. E. Joseph, N. D. Ginder, J. A. Hoy, J. C. Nix, D. B. Fulton, R. B. Honzatko, A. H. Andreotti, Structure of the interleukin-2 tyrosine kinase Src homology 2 domain; comparison between X-ray and NMR-derived structures. *Acta Crystallogr. Sect. F Struct. Biol. Cryst. Commun.* **68**, 145–153 (2012).
45. A. P. Benfield, B. B. Whiddon, J. H. Clements, S. F. Martin, Structural and energetic aspects of Grb2-SH2 domain-swapping. *Arch. Biochem. Biophys.* **462**, 47–53 (2007).
46. Z. Ahmed, Z. Timsah, K. M. Suen, N. P. Cook, G. R. Lee IV, C.-C. Lin, M. Gagea, A. A. Marti, J. E. Ladbury, Grb2 monomer-dimer equilibrium determines normal versus oncogenic function. *Nat. Commun.* **6**, 7354 (2015).
47. H. Liu, Y. R. Thaker, L. Stagg, H. Schneider, J. E. Ladbury, C. E. Rudd, SLP-76 sterile α motif (SAM) and individual H5 α helix mediate oligomer formation for microclusters and T-cell activation. *J. Biol. Chem.* **288**, 29539–29549 (2013).
48. N. P. Coussens, R. Hayashi, P. H. Brown, L. Balagopalan, A. Balbo, I. Akpan, J. C. D. Houtman, V. A. Barr, P. Schuck, E. Appella, L. E. Samelson, Multipoint binding of the SLP-76 SH2 domain to ADAP is critical for oligomerization of SLP-76 signaling complexes in stimulated T cells. *Mol. Cell. Biol.* **33**, 4140–4151 (2013).
49. T. G. M. Schmidt, L. Batz, L. Bonet, U. Carl, G. Holzapfel, K. Kiem, K. Matulewicz, D. Niermeier, I. Schuchardt, K. Stanar, Development of the Twin-Strep-tag® and its application for purification of recombinant proteins from cell culture supernatants. *Protein Expr. Purif.* **92**, 54–61 (2013).
50. W. S. Pear, J. P. Miller, L. Xu, J. C. Pui, B. Soffer, R. C. Quackenbush, A. M. Pendergast, R. Bronson, J. C. Aster, M. L. Scott, D. Baltimore, Efficient and rapid induction of a chronic myelogenous leukemia–like myeloproliferative disease in mice receiving P210 bcr/abl-transduced bone marrow. *Blood* **92**, 3780–3792 (1998).
51. R. N. Day, M. W. Davidson, The fluorescent protein palette: Tools for cellular imaging. *Chem. Soc. Rev.* **38**, 2887–2921 (2009).
52. A. Weiss, J. D. Stobo, Requirement for the coexpression of T3 and the T cell antigen receptor on a malignant human T cell line. *J. Exp. Med.* **160**, 1284–1299 (1984).
53. F. W. Studier, Protein production by auto-induction in high-density shaking cultures. *Protein Expr. Purif.* **41**, 207–234 (2005).
54. M. Hubsman, G. Yudkovsky, A. Aronheim, A novel approach for the identification of protein–protein interaction with integral membrane proteins. *Nucleic Acids Res.* **29**, E18 (2001).
55. T. Wasserman, K. Katsenelson, S. Daniliuc, T. Hasin, M. Choder, A. Aronheim, A novel c-Jun N-terminal kinase (JNK)-binding protein WDR62 is recruited to stress granules and mediates a nonclassical JNK activation. *Mol. Biol. Cell* **21**, 117–130 (2010).
56. P. O. Krutzik, M. R. Clutter, A. Trejo, G. P. Nolan, *Current Protocols in Cytometry* (John Wiley & Sons Inc., 2011).
57. T. Kambayashi, M. Okumura, R. G. Baker, C.-J. Hsu, T. Baumgart, W. Zhang, G. A. Koretzky, Independent and cooperative roles of adaptor molecules in proximal signaling during FcεRI-mediated mast cell activation. *Mol. Cell. Biol.* **30**, 4188–4196 (2010).
58. T. Kortemme, D. Baker, A simple physical model for binding energy hot spots in protein–protein complexes. *Proc. Natl. Acad. Sci. U.S.A.* **99**, 14116–14121 (2002).
59. T. Kortemme, D. E. Kim, D. Baker, Computational alanine scanning of protein-protein interfaces. *Sci. STKE* **2004**, pl2 (2004).
60. T. A. P. de Beer, K. Berka, J. M. Thornton, R. A. Laskowski, PDBsum additions. *Nucleic Acids Res.* **42**, D292–D296 (2014).

Acknowledgments: The Biomedical Core Facility (BCF) of the Rappaport Faculty of Medicine provided access to advanced FACS and ITC equipment, and BCF staff members O. Shenkar, A. Grau, and Y. Sakuory provided excellent technical support. We thank C. J. McGlade (University of Toronto) and the members of her laboratory for provision of Gads-deficient mice and for expert advice concerning the growth and maintenance of primary BMMCs; A. Stanhill for the anti-GFP antibody; R. Shofti and her staff for their professional assistance with the care and housing of our mice; O. Tabachnikov and M. Landau (Technion Faculty of Biology) for help with the SEC-MALS analysis; F. Martinpott for his contribution to this project as part of his internship program with Goettingen University; and J. Sabin (AFFINImeter) and Y. Savir (Technion) for helpful advice concerning data analysis and presentation. **Funding:** This research was supported by grants to D.Y. from the Israel Science Foundation (1368/13), the State of Lower Saxony–Israel Collaborative Fund (ZN2828), the Colleck Research Fund, and by a subsidy to D.Y. from the Russell Berrie Nanotechnology Institute. M.P.F was supported by a Cancer Research Institute Irvington Fellowship and in part by NIH grant P01 AI091580. **Author contributions:** S.S. and C.W.-L. designed and performed biochemical and biophysical experiments using recombinant Gads, with assistance from R.A., and wrote parts of the paper. M.P.F. designed the computational research, performed structural and mathematical calculations, analyzed the computational data, and wrote parts of the paper. E.H. designed, performed, and interpreted the RRS experiments under the supervision of A.A. T.I. performed, analyzed, and interpreted the BMMC experiments. R.S. made the Gads-GFP constructs and performed T cell experiments, together with D.B. I.O. developed the barcoding protocol and assisted with data analysis. E.L. generated the MBP-Gads construct and made the initial observation of Gads dimerization under the supervision of O.L. D.Y. conceived of and supervised the work and the data analysis and wrote parts of the paper. **Competing interests:** The authors declare that they have no competing interests.

Submitted 10 October 2016
Resubmitted 3 April 2017
Accepted 8 September 2017
Published 26 September 2017
10.1126/scisignal.aal1482

Citation: S. Sukenik, M. P. Frushicheva, C. Waknin-Lellouche, E. Hallumi, T. Ifrach, R. Shalah, D. Beach, R. Avidan, I. Oz, E. Libman, A. Aronheim, O. Lewinson, D. Yablonski, Dimerization of the adaptor Gads facilitates antigen receptor signaling by promoting the cooperative binding of Gads to the adaptor LAT. *Sci. Signal.* **10**, eaal1482 (2017).

Science Signaling

Dimerization of the adaptor Gads facilitates antigen receptor signaling by promoting the cooperative binding of Gads to the adaptor LAT

Sigalit Sukenik, Maria P. Frushicheva, Cecilia Waknin-Lellouche, Enas Hallumi, Talia Ifrach, Rose Shalah, Dvora Beach, Reuven Avidan, Ilana Oz, Evgeny Libman, Ami Aronheim, Oded Lewinson and Deborah Yablonski

Sci. Signal. **10** (498), eaal1482.
DOI: 10.1126/scisignal.aal1482

Gads' commitment to signaling

Binding of antigen to cell surface receptors on immune cells stimulates the formation of multiprotein complexes (signalosomes) that center around adaptor proteins, such as LAT, and are mediated by the interactions of Src homology 2 (SH2) domain–containing proteins with phosphotyrosine residues in LAT. Despite having only one SH2 domain, the adaptor protein Gads preferentially binds to LAT molecules that have more than one phosphotyrosine. Through biochemical studies and mathematical modeling, Sukenik *et al*. showed that constitutive dimerization of Gads through its SH2 domain enabled this adaptor to discriminate between singly and multiply phosphorylated LAT proteins. Disruption of the Gads dimerization interface impaired antigen receptor signaling in T cells and mast cells. These data suggest that through dimerization, Gads commits to forming signalosomes around fully phosphorylated LAT molecules, thus promoting antigen receptor responsiveness.